

Spatio-temporal Reallocation Method for Energy Management in Edge Data Centers

Junlong Li, Chenghong Gu, Lurui Fang, Xiangyu Wei, Yuanbin Zhu,
and Yue Xiang, *Senior Member, IEEE, Senior Member, CSEE*

Abstract—Edge data centers (EDCs) have been widely developed recently to supply delay-sensitive computing services, which impose prohibitively increasing electricity costs for EDC operators. This paper presents a new spatiotemporal reallocation (STR) method for energy management in EDCs. This method uses spare resources, including servers and energy storage systems (ESSs) within EDCs to reduce energy costs based on both spatial and temporal features of spare resources. This solution: 1) reallocates flexible workload between EDCs within one cluster; and 2) coordinates the electricity load of data processing, ESSs and distributed energy resources (DERs) within one EDC cluster to gain benefits from flexible electricity tariffs. In addition, this paper for the first time develops a Bit-Watt transformation to simplify the STR method and represent the relationship between data workload and electricity consumption of EDCs. Case studies justifying the developed STR method delivers satisfying cost reductions with robustness. The STR method fully utilized both spatial and temporal features of spare resources in EDCs to gain benefits from 1) varying electricity tariffs, and 2) maximumly consuming DER generation.

Index Terms—Edge data centers, electricity costs reduction, power control, power market, workload migration.

I. INTRODUCTION

ACCOMMODATED by 5G technologies, the requirement for ultra-reliable, low-delay and high-security computing services is recently growing rapidly on the edge side - edge computing (EC) [1], [2]. To meet these needs, the extension of international data centres (IDCs), edge data centres (EDCs) are being widely deployed for edge users [3]–[7]. At present, a mesh network of 100 EDCs with 6.3 MW each in the UK is under construction, targeting 7000 sites over the next 5 years [6]. Power consumption of EC in China is predicted to reach 39 GW by 2025 [8]. Power demand of EDCs is one main contributor to total EC power consumption, as each EDC consumes approximately 18–55 MW per year [9]. It, therefore, raises a problem for EDC operators in how to efficiently reallocate resources in EDCs to minimize electricity costs.

Manuscript received March 28, 2022; revised May 29, 2022; accepted October 12, 2022. Date of online publication August 19, 2020; date of current version February 9, 2024.

J. Y. Li, C. H. Gu (corresponding author, email: cg277@bath.ac.uk) and Y. B. Zhu are with University of Bath, Bath BA27AY, UK.

L. R. Fang is with Department of Electrical and Electronic Engineering, Xi'an Jiaotong-Liverpool University, Suzhou 215123, China.

X. Y. Wei and Y. Xiang are with College of Electrical Engineering, Sichuan University, Chengdu 610065, China.

DOI: 10.17775/CSEEJPES.2022.02000

Many studies have addressed the electricity cost problem for IDCs to support reliable operations of Internet online services [10]. References [10]–[12] developed workload migration methods to reduce electricity costs, where the workload is distributed between different IDCs. Thus, IDCs in low-electricity-price locations can take up more workload to reduce total costs. Reference [13] utilized an energy storage system (ESS) to reduce peak load and enable data centers to participate in power markets. Reference [14] studied the economic value of data centers integrated with distributed energy resources (DERs) as a virtual power plant. Reference [15] combined EDC clusters into a power control model of IDCs to share computing resources with IDCs. However, internal cooperation between EDC clusters (a group of EDCs in a city or area) was missing and the workload from IDCs could bring too much computing pressures to EDCs.

The scale, location, operation and distribution characteristics of IDCs and EDCs are very different [3].

- The scales of EDCs are much smaller than IDCs. With fewer customers and smaller coverage ranges, the workload for EDCs could be more unstable with significant fluctuations. This brings difficulties for workload prediction for EDCs, thus high robustness of workload dispatching is required.
- Small scale of EDCs also leads to more significant differences between workload amounts in different EDCs. EDCs for commercial customers and residential customers could lead to very different workload amounts over time, which brings more value for workload migration between them.
- Geographical distance between EDCs in one cluster is much shorter than between IDCs, leading to an ignorable communication delay between EDCs.
- The number of EDCs in a city could be large with different operators. Thus, optimisation could be time-consuming with a high dimension of decision variables.

These differences imply that existing bespoke approaches for reducing electricity costs of IDCs are not fully applicable to EDCs. A customised approach is required to accommodate EDCs with different characteristics to reduce electricity costs. Since price differences still exist for EDCs that are 1) operated by different companies, and 2) connected to different transmission buses or voltage levels of distribution networks, workload migration still has huge value for EDC clusters. Furthermore, compared with IDCs, short transmission delay

between EDCs in the same cluster provide more conveniences and higher feasibility for workload migration.

To address the above problems, this paper presents a spatiotemporal reallocation (STR) method to reduce electricity costs in EDCs. It first proposes a power consumption model for EDCs, which contains a Bit-Watt transformation that reveals the relationship between workload and power consumption of EDCs. Then, a STR method is developed for EDC clusters, which has four steps: 1) scheduling day-ahead workload migration on a special dimension to reduce electricity costs; 2) optimising ESS operation on the temporal dimension to gain benefits from flexible electricity time-of-use tariffs; 3) rescheduling ESS and reallocating workflow between EDCs to maximally consume local DERs; 4) adjusting workload migration between EDCs according to real-time data arriving rate.

Main optimisation on spatial and temporal dimension are decoupled and performed by stages 1 and 2, only redundant DER tracking requires spatiotemporal optimisation in stage 3. This simplifies the optimisation complexity by solving several sub-optimisations with a small dimension of variables. Stage 4 can effectively avoid errors of workload prediction in EDCs, which is essential for robustness of workload migration among EDCs [16]. The proposed method is tested on a 15-EDC cluster with different electricity tariffs. Results justify the efficiency and robustness of the proposed method in electricity cost reduction for EDCs.

It should be noted the energy storage (ES) capacity for the Uninterrupted Power Supply (UPS) is not included in the STR method. Since the newly built EDCs tend to be constructed in a multi-station mode with ES stations [3]–[5], [7], the ESS resource in EDCs is valuable to reduce electricity costs for its flexibility of load shifting [17]. Therefore, the EDCs with or without ESSs are all considered in the STR method to maximumly utilize resources in EDC clusters. In addition, EDCs could be operated by different operators, thus a third-party entity is assumed to be responsible to perform this STR method. This entity can coordinate different EDCs to minimise their power cost and charge a service fee.

The innovations of the paper are as follows:

- This paper for the first time considers both the spatial and temporal features of spare resources (servers and ESSs) in EDCs to obtain economic benefits from varying local electricity tariffs. Comparatively, the spatial and temporal features are separately optimized in the workload migration and energy management respectively, in traditional ways for IDCs.
- A rolling adjustment stage is developed in the STR method to resolve high uncertainty in workload furcating for EDCs, which can enhance robustness of optimisation

with safety margins by considering real-time changes in the workload migration optimization.

- To reduce the number of decision variables in the optimization of EDC clusters, a novel Bit-Watt transformation is developed in the STR method, which models the relationship between EDC power consumption and computing workload amount. Besides, optimisation is decoupled into spatial and temporal dimensions in stages 1–3 to reduce the dimension of decision variables.

The rest of this paper is organised as follows: The background and definition of EDCs are presented in Section II. The EDC energy consumption model with Bit-Watt transformation is developed in Section III. Section IV presents the proposed STR method. A case study of the proposed method and related analysis are presented in Section V. The conclusion is summarised in Section VI.

II. BACKGROUND AND DEFINITION OF EDCS

Many EDCs have been constructed or under-construction [3]–[7], where the largest EDC can consume 250 times the electricity of the smallest one. To reduce analysis complexity, we categorise EDCs into 3 groups in Table I according to 1) the position paper ‘edge data centers’ of Telecommunications Industry Association claimed the operation power of EDCs ranges from 50 to 150 KW, so a regular EDC is defined according to it [9], and 2) the number of EDCs per million population is based on [18] according to the equipment size of EDCs. Considering supersized EDCs can be operated as IDCs and micro-EDCs are deployed with very limited servers, this paper mainly focuses on regular EDCs, which are centrally controlled by EDC operators.

By combining the common features and possible devices of different EDCs [3], [4], [6], [7], the hardware structure of EDC is shown in Fig. 1. The IT equipment, cooling system and other devices are the main electricity load in EDCs. There are two flows within EDCs: power and data.

- For power flows, energy from the distribution network and DERs are consumed by EDC devices or stored by ESS.
- For data flows, the workload, which could be from local users, front portal, and other EDCs, is received by network devices and processed by servers.

Other multi-station loads like base stations possibly exist in EDCs, decided by the scale and operators of EDCs. Besides, for EDCs with a high proportion of DERs, generation could be larger than EDC power load, which decreases operation economy of EDCs if residual DERs cannot be sold to the power grid. Thus, how to reallocate spare servers and ESSs in EDC clusters to consume residual DERs is important to investigate in the STR method.

TABLE I
CLASSIFICATION OF EDCS WITH TYPICAL REAL EXAMPLES

Classification of EDC	Maximum power	Size	EDCs/million population	Example
Supersize EDC	150+ KW	10+ racks	1 EDC	Proximity Data Centres Ltd.
Regular EDC	50–150 KW	2–10 racks	15 EDCs	American Tower
Micro-EDC	50 KW max	2 racks max	300 EDCs	RISE ICE Datacentres research facility

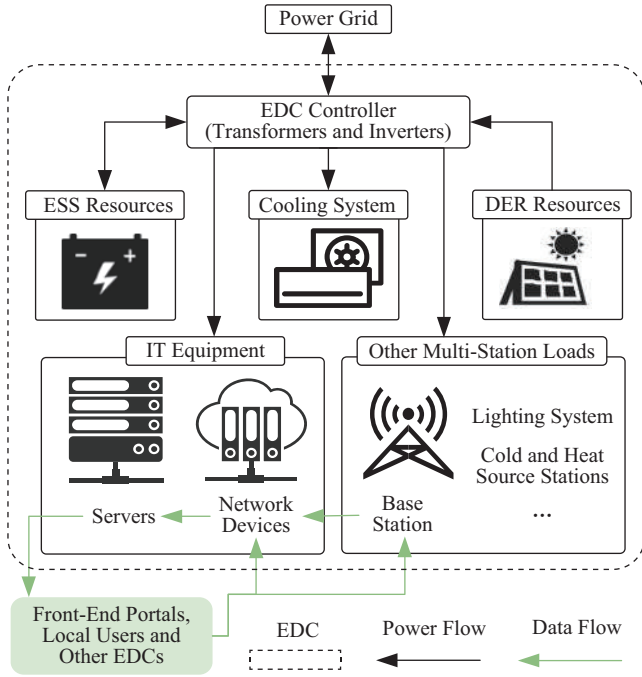


Fig. 1. The hardware structure for EDCs.

III. WORKLOAD-BASED POWER CONSUMPTION IN EDCs

This section develops a workload-based power consumption model for EDCs. First, Section A develops a power consumption model of EDCs based on the number of active servers. Section B develops a Bit-Watt transformation to obtain power consumption in any EDC from the server workload. This transformation reveals the relationship between workload amount and energy consumption within EDCs. The STR optimization model only requires workload amount as the decision variable, thus simplifying the optimization. Section C formulates the workload-based power consumption of EDCs.

A. Power Consumption Modeling for EDCs

Power consumption of i^{th} EDC at the t^{th} time slot, $L_{\text{EDC}_i}^t$, can be divided into two parts: real loads related to the number of active servers and possible loads irrelevant to the number of active servers, as shown in (1). In this paper, t means the t^{th} time slot and is written as the superscripts of the variables. The servers power consumption $L_{\text{Ser}_i}^t(n_i^t)$ is decided by n_i^t , the number of active servers of i^{th} EDC at the t^{th} time slot [10], defined in (2). Power consumption caused by network devices $L_{\text{Net}_i}^t(n_i^t)$ can be presented by a linear function in (3) with coefficients α_{Net_i} and β_{Net_i} . This is based on the k -ary fat-tree, which is a widely used three-layer topology (edge, aggregation and core) for switches [19], [20]. Power consumption of the cooling system $L_{\text{Cool}_i}^t(n_i^t)$ is obtained by (4) based on a joint cooling strategy [21], [22] that utilizes external-internal air circulation.

$$\begin{aligned} L_{\text{EDC}_i}^t &= L_{\text{Ser}_i}^t(n_i^t) + L_{\text{Net}_i}^t(n_i^t) + L_{\text{Cool}_i}^t(n_i^t) \\ &\quad + \mu_{i\varphi}(L_{\text{Adt}_i}^t + L_{\text{CES}_i}^t - G_{\text{DES}_i}^t - G_{\text{DER}_i}^t) \\ &= L_{\text{RSer}_i}^t(n_i^t) + \mu_i L_{\text{NSer}_i}^t \end{aligned} \quad (1)$$

$$\forall i \in I, t \in T, n_i^t \in N_i, \mu_{i\varphi} \in \begin{bmatrix} \mu_{1ES} & \mu_{1DER} & \mu_{1Adt} \\ \mu_{2ES} & \mu_{2DER} & \mu_{2Adt} \\ \dots & \dots & \dots \\ \mu_{IES} & \mu_{IDER} & \mu_{IAdt} \end{bmatrix}$$

$$L_{\text{Ser}_i}^t(n_i^t) = (\gamma_i f_i^{\varepsilon_i} + \delta_i) n_i^t \quad (2)$$

$$L_{\text{Net}_i}^t(n_i^t) = \alpha_{\text{Net}_i} n_i^t + \beta_{\text{Net}_i} \quad (3)$$

$$L_{\text{Cool}_i}^t(n_i^t) = \text{coe}_i (L_{\text{Ser}_i}^t(n_i^t) + L_{\text{Net}_i}^t(n_i^t) + H_i^t) \quad (4)$$

where, $L_{\text{Adt}_i}^t$ and $L_{\text{CES}_i}^t$ are the power consumption of additional other multi-station loads (shown in Fig. 1), and ES charging, respectively, in the i^{th} EDC at the t^{th} time slot, $G_{\text{DES}_i}^t$ and $G_{\text{DER}_i}^t$ are the power output from ES discharging and DERs, $L_{\text{RSer}_i}^t$ and $L_{\text{NSer}_i}^t$ are the real loads and possible loads, μ_i is a matrix to represent the existence of multi-station resources. N_i is the total number of servers in i^{th} EDC, I is the number of EDCs in the distribution network, T is the scheduling period, f_i is the average CPU frequency of servers, ε_i , γ_i and δ_i are constant coefficients, coe_i is the cooling efficiency defined as heat removed by the cooling systems and relative to power consumption, H_i^t is the heat from ES and other devices in a multi-station mode.

B. Bit-Watt Transformation in EDCs

To reduce electricity costs, the developed STR method reallocates workload between EDCs. However, in (1)–(4), the variable for calculating power consumption is the number of active servers, not the magnitude of workload. In the power consumption model for EDCs, therefore, the number of active servers should be replaced by the workload.

This section develops a Bit-Watt transformation. It reveals the relationship between workload and power consumption for any EDC. According to M/M/n queueing theory [10], [23], workload processing time $T_{\text{pro}_i}^t$ is described by the number of active servers, CPU frequency and workload, as shown in (5)–(6) with constraints in (7)–(9). The M/M/n queueing theory is a multi-server queueing model governed by a Poisson process.

$$T_{\text{pro}_i}^t = \frac{1}{\vartheta_i f_i n_i^t - \lambda_i^t}, \quad \forall i \in I, t \in T, n_i^t \in N_i \quad (5)$$

$$\lambda_i^t = \sum_{j=1}^J \lambda_{ij}^t + \lambda_{i0}^t + \sum_{x=1}^I \lambda_{ix}^t - \sum_{x=1}^I \lambda_{xi}^t, \quad x \neq i \quad (6)$$

$$0 < T_{\text{pro}_i}^t \leq \overline{\text{Delay}_i} \quad (7)$$

$$\sum_{i=1}^I \sum_{j=1}^J \lambda_{ij}^t = \lambda_{\text{Ser}}^t, \quad \sum_{i=1}^I \lambda_{i0}^t = \lambda_{\text{EDC}}^t \quad (8)$$

$$\sum_{i=1}^I \lambda_i^t = \lambda_{\text{Ser}}^t + \lambda_{\text{EDC}}^t = \lambda_{\text{Total}}^t \quad (9)$$

where, λ_{ij}^t and λ_{ix}^t are the migrated workload from front-end portal server j and x^{th} EDC to i^{th} EDC at t^{th} time slot, ϑ_i is the frequency efficiency to convert CPU frequency into server service rate, J is the total number of front-end web portal servers, λ_{i0}^t is the workload from local users, λ_{Total}^t is the total shiftable workload amount at t^{th} time slot, $\overline{\text{Delay}_i}$ is the maximum processing delay.

Given that $T_{pro_i}^t > 0$, (5) is converted to (10). Considering the number of active servers is an integer (10) is an approximate formula. Second, since the derivative of n_i^t with respect to $T_{pro_i}^t$ is negative as shown in (11), the number of active servers decreases with increasing processing time. In addition, power load related to the number of active servers increases with the increasing number of active servers, as proved by (12). Therefore, inequality (13) holds. Thus, with increasing data processing time, electricity consumption decreases. This implies that if the processing time equals the allowed maximum processing delay, electricity consumption is minimal, as shown in (14).

$$n_i^t \approx (1 + \lambda_i^t T_{pro_i}^t) (\vartheta_i f_i T_{pro_i}^t)^{-1} \quad (10)$$

$$\frac{\partial n_i^t}{\partial T_{pro_i}^t} = -\frac{1}{\vartheta_i f_i T_{pro_i}^t{}^2} \leq 0 \quad (11)$$

$$\frac{\partial L_{R_{Ser}_i^t}(n_i^t)}{\partial n_i^t} = (coe_i + 1) (\gamma_i f_i^{\varepsilon_i} + \delta_i + \alpha_{Net_i}) \geq 0 \quad (12)$$

$$L_{R_{Ser}_i^t}(n_i^t) \geq L_{R_{Ser}_i^t} \left(\frac{1 + \lambda_i^t \overline{\text{Delay}_i}}{\vartheta_i f_i \overline{\text{Delay}_i}} \right) \quad (13)$$

$$\min L_{R_{Ser}_i^t}(n_i^t) \xrightarrow{T_{pro_i}^t = \overline{\text{Delay}_i}} \min L_{R_{Ser}_i^t}(\lambda_i^t) \quad (14)$$

C. Workload-Based Power Consumption Model

Based on the Bit-Watt transformation, the minimum power consumption of EDCs is converted as the workload-based power consumption model by combining (1)–(4), (10) and (14), as shown in (15). This formula is linear with constant coefficients a_i and b_i in (16)–(17), which can be obtained by other constant coefficients. In this way, EDC power consumption is calculated by the workload amount directly.

$$\min L_{R_{Ser}_i^t} = \min (a_i \lambda_i^t + b_i) \quad (15)$$

$$a_i = \frac{(coe_i + 1) (\gamma_i f_i^{\varepsilon_i} + \delta_i + \alpha_{Net_i})}{\vartheta_i f_i} \quad (16)$$

$$b_i = \frac{(coe_i + 1) (\gamma_i f_i^{\varepsilon_i} + \delta_i + \alpha_{Net_i})}{\vartheta_i f_i \overline{\text{Delay}_i}} + (coe_i + 1) \beta_{Net_i} + coe_i H_i^t \quad (17)$$

IV. FORMULATION OF STR METHOD FOR EDCS

This section develops an STR method to optimally manage power flows between EDCs to achieve minimal electricity costs for an EDC cluster. The STR method contains 4 main stages as shown in Fig. 2.

- Stage 1 schedules the day-ahead workload migration scheme to allocate workload between EDCs to obtain minimum electricity costs within one EDC cluster.
- Stage 2 optimises ESS discharging at a high-price period and charging at a low-price period. Meanwhile, ESS is discharged at peak periods and charged at off-peak periods for any EDC.
- Stage 3 reallocates EDCs' power consumption to follow local DER generation to consume DER generation locally. The developed spatiotemporal DER tracking method utilizes available ESSs and free servers in other EDCs to follow DER output, as much as possible.

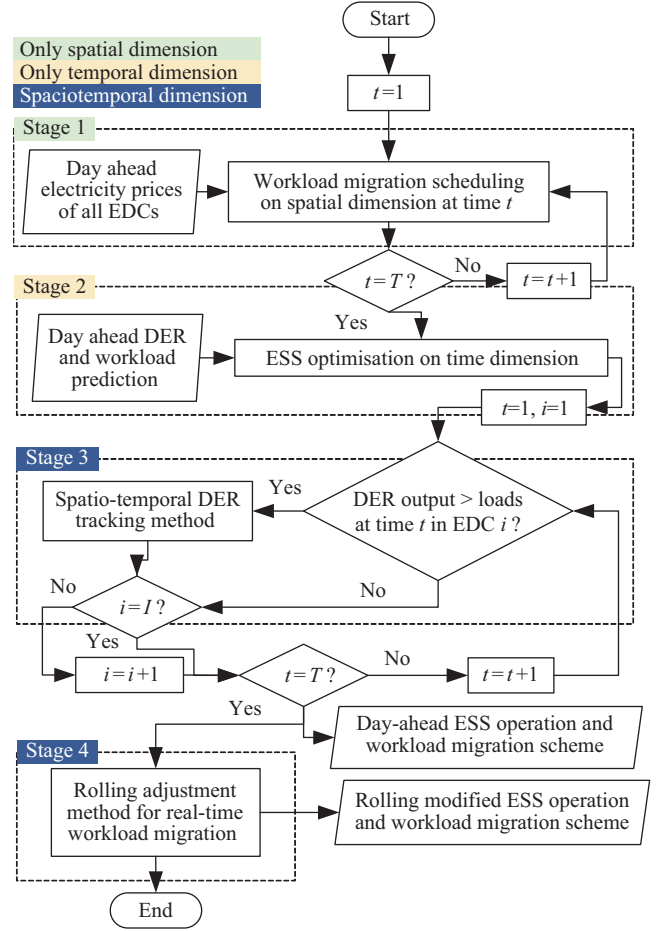


Fig. 2. The framework of the STR method.

- Stage 4 performs a rolling-based adjustment method to guarantee all workload is timely processed, although under unexpected extreme scenarios, e.g., EDCs workload accidentally skyrockets.

Stage 1 and 2 provide the basic solution for operation of ESS and workload, and Stage 3 and 4 are a crucial supplement to stages 1 and 2. Specifically, stage 3 enables a developed method to fully consume possible wasted DER generation in previous stages, while stage 4 provides real-time adjustment to avoid the effects of inaccurate workload prediction. For the 4 stages of the STR method, spatial, temporal and both spatial and temporal (Spatiotemporal) dimensions are considered. These three dimensions promote efficiency in reducing electricity costs and maximally consuming residual DER locally. The detailed benefits of the four stages will be demonstrated and discussed in the case study in Section V.

A. Optimization of Workload Migration

This section defines the cost function for applying workload migration. Workload reallocated from one EDC to another could bring additional costs. Suppose there are two EDCs, A and B, owned by different operators. When the workload is migrated from A to B, A should pay B the marginal workload cost $Pri_{\lambda_x}^t$ and additional server rent fee Pri_{Ad_x} . If the communication bandwidth between two EDCs is occupied, it leads to

additional bandwidth usage fees for EDC A. Third, workload migration also brings additional communication delay to EDC users, which may cause additional costs for EDC operators.

Bandwidth usage and delay-caused costs are decided by communication distance Dis_{xi}^t between EDCs. Thus, the costs of workload migration at t^{th} time slot for the i^{th} EDC, $C_{WM_i}^t$, is given by (18). $Pri_{\lambda_x}^t$ is the marginal workload cost for the x^{th} EDC ($x \neq i$) at the t^{th} time slot. In this paper, the marginal workload cost is set to the incremental electricity cost for the EDC that receives migrated workload, as shown in (19).

$$C_{WM_i}^t = \sum_{x=1}^I \lambda_{xi}^t (Pri_{\lambda_x}^t + Pri_{Ad_x} + Dis_{xi}^t C_{BD_{xi}}^t) - \sum_{x=1}^I \lambda_{ix}^t (Pri_{\lambda_i}^t + Pri_{Ad_i}) \quad (18)$$

$$Pri_{\lambda_x} = Pri_{E_x}^t \frac{\partial L_{EDC_x}}{\partial \lambda_x^t} = Pri_{E_x}^t a_x \quad (19)$$

where, $C_{BD_{xi}}^t$ is the unit cost of bandwidth occupation and additional delay between the x^{th} and the i^{th} EDC.

By combining (15)–(17) and the workload migration costs in (18), the optimization objective function of day-ahead workload migration scheduling on spatial dimension is given by (20). It is subjected to the constraints of available server numbers, total workload amount and extremely time-sensitive or privacy-sensitive workload amounts, given in (22)–(24). $\mu_{fix_i}^t$ is the proportion of the extremely delay-sensitive or privacy-sensitive workloads to the total workload at the i^{th} EDC at the t^{th} time slot.

$$f_{Stage1} = \sum_{t=1}^T f_{WM}^t \quad (20)$$

$$\begin{aligned} f_{WM}^t &= \min \sum_{i=1}^I (Pri_i^t L_{EDC_i}^t + C_{WM_i}^t) \\ &= \min \sum_{i=1}^I (Pri_i^t L_{R_{Ser}_i}^t (\lambda_i^t) + C_{WM_i}^t (\lambda_i^t)) \\ &\quad + \sum_{i=1}^I Pri_i^t \mu_i L_{NSer_i}^t \end{aligned} \quad (21)$$

$$\text{s.t. } (1 + \lambda_i^t \overline{\text{Delay}_i}) (\vartheta f_i \overline{\text{Delay}_i})^{-1} \leq N_i \quad (22)$$

$$\sum_{i=1}^I \lambda_i^t \geq \lambda_{\text{Total}}^t \quad (23)$$

$$\lambda_i^t \geq \mu_{fix_i}^t \left(\sum_{j=1}^J \lambda_{ij}^t + \lambda_i^t \right) \quad (24)$$

B. Optimization of ESS

The objective for ESS operation aims to reduce electricity costs and peak load, as shown in (25). μ_{ESS} is a coefficient to ensure that when minimizing the secondary objective f_{ESS2} , it will not affect the results of the main objective f_{ESS1} . f_{ESS1} is to utilize the price variations on different time slots to gain profits, presented in (26). Thus, the secondary optimisation

objective is to locally consume DERs and reduce peak load for having a lower network price for EDCs, as given by (27). The optimization of ESS is subjected to the capacity, emergency margin, power balance and charging/discharging rate of batteries as in (28)–(32).

$$f_{Stage2} = f_{ESS1} + \mu_{ESS} f_{ESS2} \quad (25)$$

$$f_{ESS1} = \min \sum_{t=1}^T Pri_{E_x}^t (L_{CES_i}^t - G_{DES_i}^t) \quad (26)$$

$$f_{ESS2} = \min \sum_{t=1}^T (L_{EDC_i}^t + L_{CES_i}^t - G_{DES_i}^t)^2 \quad (27)$$

$$\text{s.t. } \underline{\text{SoC}_i} \leq \sum_{w=1}^t L_{CES_i}^w \eta_{C_i} - \sum_{w=1}^t \frac{G_{DES_i}^w}{\eta_{D_i}} \leq \overline{\text{SoC}_i}, w \in T \quad (28)$$

$$\sum_{w=1}^t L_{CES_i}^w \eta_{C_i} - \sum_{w=1}^t \frac{G_{DES_i}^w}{\eta_{D_i}} \geq \underline{\text{EM}_i} \quad (29)$$

$$\sum_{t=1}^T L_{CES_i}^t \eta_{C_i} = \sum_{t=1}^T \frac{G_{DES_i}^t}{\eta_{D_i}} \leq \overline{\text{SoC}_i} \quad (30)$$

$$\sum_{t=1}^T |L_{CES_i}^t G_{DES_i}^t| = 0 \quad (31)$$

$$L_{CES_i}^t \leq \overline{R_{CES_i}}, G_{DES_i}^t \leq \overline{R_{DES_i}} \quad (32)$$

where, f_{stage2} , f_{ESS1} and f_{ESS2} are the total, main, and secondary objective function of ESS optimization on the temporal dimension, η_{C_i} and η_{D_i} are the charging and discharging efficiency of ESS in i^{th} EDC, $\overline{\text{SoC}_i}$ and $\underline{\text{SoC}_i}$ are the maximum and minimum of the ESS SoC, $\overline{R_{CES_i}}$ and $\overline{R_{DES_i}}$ are the charging and discharging rate of the ESS, $\underline{\text{EM}_i}$ is the energy margin for the UPS in i^{th} EDC.

C. Spatiotemporal DER Tracking Method

This section develops a DER tracking method for rescheduling ESS operations and mitigating workload on both temporal and spatial dimensions on a day-ahead basis. There are many ways to consume residual generation from local DERs for EDCs, such as increasing EDC workload and rescheduling the ESS operation scheme. This section defines the cost function for EDCs. Suppose the i^{th} EDC has residual DER generation at a given time slot. Reallocating workload and rescheduling ESS bring the following costs and benefits:

1) If the i^{th} EDC is scheduled to send its workload to other EDCs, cancelling sending a given amount of the workload saves overall electricity costs and workload migration cost for the i^{th} EDC, as given by (33).

2) Allocating more workload from other EDCs to the i^{th} EDC to consume DER's residual generation and prevent purchasing electricity from the grid for other EDCs. However, workload migration costs increase when transferring the workload from other EDCs to the i^{th} EDC. The cost function is given by (34).

3) Rescheduling the operation scheme of the i^{th} EDC's ESS to consume local residual generation, thus gaining benefits from flexible electricity tariffs, e.g., time of use tariffs (TOU). The cost function is given by (35) and (36).

Thus, this section is to find an optimal way to absorb the residual DERs with maximum profits or minimum costs as shown in (37) with constraints (39)–(40).

$$\Delta C_{1i}^t = - \sum_{x=1}^I \Delta \lambda_{xi}^t (Pri_{\lambda x}^t + Dis_{xi}^t C_{BDxi}^t) \quad (33)$$

$$\Delta C_{4i}^t = - \sum_{x=1}^I \Delta \lambda_{ix}^t ((Pri_{\lambda x}^t - Dis_{ix}^t C_{BDix}^t)) \quad (34)$$

$$\Delta C_{2i}^t = - \sum_{t=1}^T \Delta L_{CESi}^t * Pri_{E_x}^t \quad (35)$$

$$\Delta C_{3i}^t = - \sum_{t=1}^T \Delta G_{DESi}^t * Pri_{E_x}^t \quad (36)$$

$$f_{Stage3} = \sum_{t=1}^T \sum_{i=1}^I \sum_{q=1}^4 \Delta C_{qi}^t \quad (37)$$

$$\text{s.t. (21)–(24), (29)–(31), and} \quad (38)$$

$$a_i \sum_{x=1}^I (\Delta \lambda_{ix}^t + \Delta \lambda_{xi}^t) + b_i + \Delta L_{CESi}^t = |\min(L_{EDCi}^t, 0)| \quad (39)$$

$$\Delta \lambda_{ix}^t \Delta \lambda_{xi}^t = 0 \quad (40)$$

D. Rolling Adjustment for Real-Time Workload Migration

Considering the error in day-ahead workload prediction, this section develops a rolling method to adjust workload in real-time. Because prediction errors are normally much less than the total workload, this method is not to reduce electricity costs but to ensure all workload is timely processed by the EDC clusters with a safety margin, i.e., safety margin here refers to a certain number of free servers in EDCs for emergency needs, such as unexpected workload explosion.

A flowchart of the proposed method is given in Fig. 3. The rolling period Δt is less than one hour, such as 5 minutes or 10 minutes. On a real-time basis, EDCs continuously calculate their duty ratio every second. The duty ratio of the x^{th} EDC at time t , ρ_x^t , is the percentage of the utilized servers in EDCs, as given by (41). If the duty ratio has not achieved its maximum value (such as 90% in this paper) during the rolling period for the x^{th} EDC, that EDC will send the number of its available

servers m_x^t to the control center at the end of the rolling period, given by (42). Then, the cloud will update the numbers of free servers for every EDC. Once ρ_x^t meets its maximum value, the extra workload will be sent to other nearby EDCs according to the number of available servers sent to the cloud node. The workload, sent from the overloaded EDC to nearby EDCs, is given by (43)–(44). Nearby EDCs with larger numbers of available servers will be proportionally reallocated with more workload to keep a certain number of available servers in all EDCs for emergency needs. $\mu_{dis_{xi}}^t$ is the distance coefficient to ensure overloaded EDCs only migrate the extra workloads to nearby EDCs for decreasing transformation delay.

$$\rho_x^t = \frac{1 + \lambda_x^t \overline{\text{Delay}}_x}{N_x \vartheta f_x \overline{\text{Delay}}_x} \times 100\% \quad (41)$$

$$m_x^t = N_x - \frac{1 + \lambda_x^t \overline{\text{Delay}}_x}{\vartheta f_x \overline{\text{Delay}}_x} \quad (42)$$

$$\lambda_{over_{xi}}^t = \lambda_{over_i}^t \frac{m_x^t \mu_{dis_{xi}}^t}{\sum_{x=1}^I m_x^t \mu_{dis_{xi}}^t} \quad (43)$$

$$\mu_{dis_{xi}}^t = \begin{cases} 0, & Dis_{xi}^t > \frac{\sum_{x=1}^I Dis_{xi}^t}{I} \\ 1, & Dis_{xi}^t \leq \frac{\sum_{x=1}^I Dis_{xi}^t}{I} \end{cases} \quad (44)$$

where, $\lambda_{over_{xi}}^t$ and $\lambda_{over_i}^t$ are the overload workload migrated from the i^{th} EDC to x^{th} EDC and the total overload workload amount in the i^{th} EDC.

V. CASE DEMONSTRATION

In this section, an EDC cluster at a city level is used to justify the proposed method. Section V-A presents the input data. Section V-B, based on the STR model, performs the optimisation result of the benchmark case without workload migration costs. Section V-C, D and E perform the efficacy of the proposed method under different scenarios: high workload migration costs, high-proportion DERs and unpredicted workload growth, respectively.

A. Input Data

This case study adopts regular EDCs, defined in Table I, in a city of one million population, where there will be 15 regular EDCs with a maximum load power of 50–150 KW. The details of EDCs are presented in Table II. Considering space limitation, the DERs are assumed as PV resources in this case demonstration. Geographical distribution of an EDC cluster can be found in Fig. 10 in Subsection V-E. EDCs, located on the lower voltage level of the distribution network, are supposed to be located closer to the city center.

Parameters of servers, network devices and cooling systems in EDCs are assumed to be equal to each other to simplify the calculation. The constant parameters $[f_i, \varepsilon, \gamma_i, \delta_i, \alpha_{Neti}, \beta_{Neti}, \vartheta_i]$ (defined in (2)–(3)) are set as $[3.4, 3, 3.206, 68, 170, 0, 1]$ according to [10], [12], [19], [24]. COE_i (defined in (4)) is assumed to be constant with the value of 0.5 [21]. $\mu_{fix_i}^t$ (defined in (24)) and L_{Adti}^t (defined in (1)) are set as 10% and 0. By combining data from HTTP requests to the NASA Kennedy Space Centre WWW server in Florida [25], the average workload arriving rate of EDCs is presented in Fig. 4.

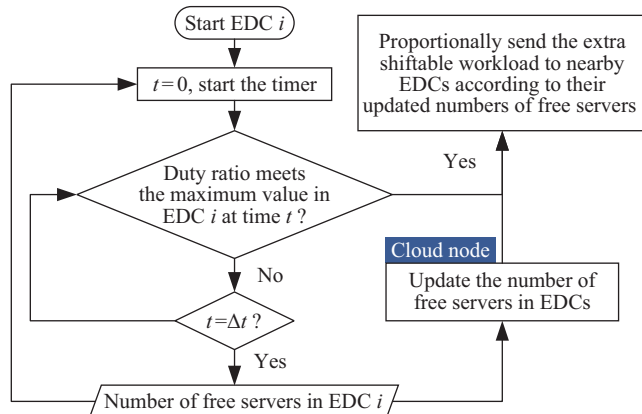


Fig. 3. Logic diagram of the rolling adjustment method.

TABLE II
DETAILED INFORMATION OF 15 EDCs

EDC number	Network voltage (kV) and electricity pricing method	Multi-station mode	Maximum power (kW)	Maximum Workload
1	10 (FPT)	None	80	465
2	10 (FPT)	None	85	496
3	10 (FPT)	None	90	527
4	10 (FPT)	None	95	558
5	10 (FPT)	None	100	589
6	10 (TOUT)	ESS	105	620
7	10 (TOUT)	ESS	110	652
8	35 (FPT)	None	115	683
9	35 (FPT)	None	120	714
10	35 (TOUT)	ESS	125	745
11	35 (TOUT)	ESS	130	776
12	35 (TOUT)	ESS	135	807
13	35 (TOUT)	ESS	140	838
14	110 (TOUT)	ESS+DER	145	870
15	110 (TOUT)	ESS+DER	150	901

The time-of-use tariff (TOUT) and fixed price tariff (FPT) are set as the real electricity price in Beijing presented in Table III.

This section studies four different cases, presented in Subsections V-B, C, D and E. The inputs setting of each case is shown as follows:

1) Benchmark case: Energy capacity and maximum charging/discharging power of the ESS is set as 60 kWh and 10 kW, respectively. \overline{Delay}_i , \overline{SoC}_i , SoC_i and \overline{EM}_i are set as 3 ms, 100%, 0% and 10 kWh. DER output in EDC 14 and 15 is set as half the DER output in Fig. 9 in Section V-D. Workload migration cost is set as ¥0.

2) Case with workload migration cost: On top of the benchmark case, this section considers workload migration cost. This cost, defined in (18), is positively correlated with the communication distance between two EDCs. Thus, workload migration cost for each 1 km is set as proportional to the average electricity costs of workload, given in (45). μ_{BD} is set between 0 and 10% to reflect the benefits of the STR method under different workload migration costs.

$$C_{BD_{xi}}^t = Dis_{xi}^t \mu_{BD} \frac{\sum_{i=1}^I Pri_{\lambda_i}^t \left(\sum_{j=1}^J \lambda_{ij}^t + \lambda_{i0}^t \right)}{\lambda_{Total}^t} \quad (45)$$

3) Case considering high-level DERs: Compared to the scenario in Section V-C, this scenario adds another additional variable – one DER with the maximum power of 120 KW – onto the energy consumption model of EDC 15 to demonstrate the economic benefits of the spatiotemporal DER tracking method. In this case μ_{BD} is set to 1%.

4) Case considering inaccurate workload predictions: The prediction of workload and DER output normally has errors. Thus, with the same inputs in the benchmark case, a number of

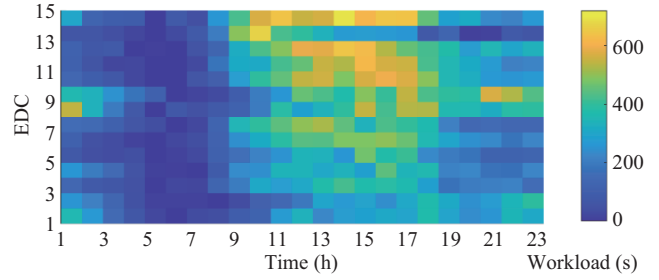


Fig. 4. Average workload arriving rate of 15 EDCs.

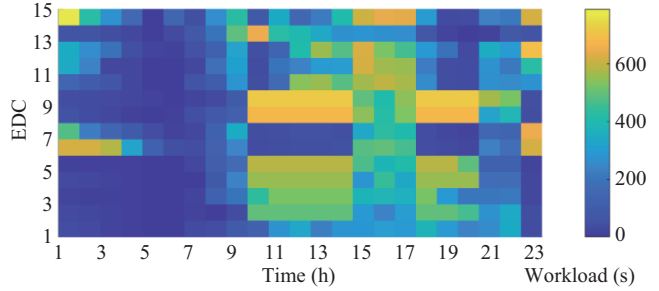


Fig. 5. Workload arriving rate of 15 EDCs optimised by the STR method.

random computing tasks, ranging from 0 to 20% of the original workload, are added into the EDC cluster as the unexpected workload. In this case μ_{BD} is set to 1%.

B. Benchmark Case

Based on rescheduling ESS operation and workload migration, the developed STR method can save 2.99% and 14.59% on electricity costs, respectively. Workload migration gains an average benefit of 2029 ¥/day for EDC operators. Fig. 5 presents an optimised workload arriving rate for 15 EDCs by the STR method. Compared with the original case in Fig. 4, the workload allocated in EDCs is more regular, as the workload is primarily allocated to EDCs with low electricity costs in each time slot. Reduced electricity consumption by migrating workload between EDCs throughout 24 hours is presented in Fig. 6 ($\mu_{BD} = 0\%$), which also indicates that electricity costs are significantly reduced with larger electricity price variations.

Since the coefficients of servers in EDCs could be various in the practical, sensitive analysis of maximum delay, \overline{Delay} and CPU frequency efficiency ϑ_i are presented in Fig. 7. These two coefficients determine how much workload can be processed by servers in EDCs. With increase of these two coefficients, electricity reduction rapidly increases then slowly converges to a certain value. This value is the ideal optimal reallocation result where all workload has been allocated to low-electricity-

TABLE III
ELECTRICITY PRICE OF INDUSTRIAL AND COMMERCIAL USERS IN BEIJING

Network voltage level (kV)	TOUT (¥/kWh)			FPT (¥/kWh)
	On-Peak (10:00–15:00; 18:00–21:00)	Medium peak (7:00–10:00; 15:00–18:00; 21:00–23:00)	Off-peak (23:00–7:00)	
1-10	1.28	0.77	0.27	0.81
35	1.26	0.75	0.25	0.79
110	1.25	0.73	0.24	0.77

price EDCs.

C. Case with Workload Migration Costs

With increasing workload migration cost, efficacy of the STR method decreases. The relationship between the percentage of electricity cost reduction percentage and workload migration costs is nearly linear with a slope of -0.75 . When $\mu_{BD} = 5\%$, the optimised workload arriving rate for each EDC and overall hourly electricity reduction are presented in Fig. 8 and 6, respectively. Because of the high migration cost for the case in Fig. 8, the optimised workload arriving rate does not achieve that of the benchmark case. Particularly, in Fig. 6 ($\mu_{BD} = 5\%$), some time slots, e.g., time slots 7th–9th, 15th–17th and 21st–22nd, do not gain electricity cost reductions. It is because, throughout those time slots, electricity price variation is not significant, and thus it is not cost-effective for EDCs to reallocate their workload to others.

Figure 9 presents the workload migration scheme for EDC 9 with $\mu_{BD} = 0$ and 5%. A workload migration scheme with 5%

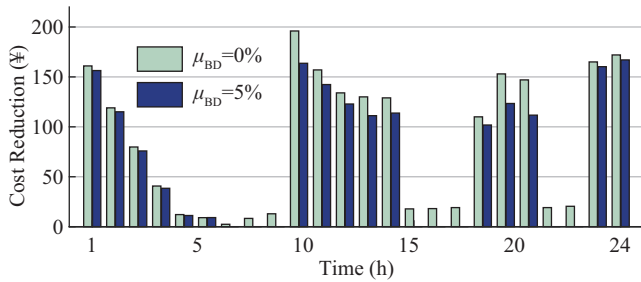


Fig. 6. Electricity cost reduction amount in the EDC cluster during 24 hours with $\mu_{BD} = 0\%$ (no workload migration costs) and 5%.

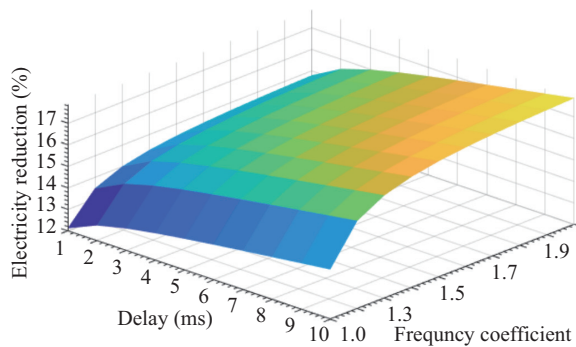


Fig. 7. Sensitive analysis of maximum delay $\overline{\text{Delay}}$ and CPU frequency efficiency ϑ_i .

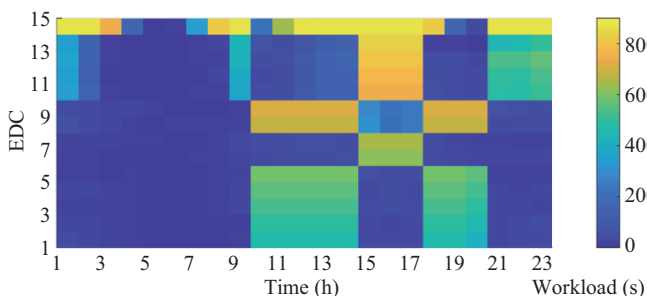


Fig. 8. Workload arriving rate of EDCs with $\mu_{BD} = 5\%$.

μ_{BD} is simpler and more regular, thus simplifying workload dispatching complexity in reality. At this time, only EDCs near EDC 9 share their workload and free server resources with EDC 9, such as EDC 6 and 10. Moreover, on the data processing side, the simplified workload migration scheme (shown in Fig. 9) also prevents higher data transmission delay compared to the benchmark case.

D. Case Considering High-Level DERs

The original load, DER output, ESS operation and DER tracking results are presented in Fig. 10. The dashed area in Fig. 10 presents that not all of DER output is utilized throughout time slots 10th–14th even if the residual DER cannot be injected into the grid. By using the DER tracking method in Subsection IV-C, residual DER output in EDC 15 can be fully absorbed by migrating workloads from other EDCs. Totally, the EDC clusters save electricity costs of ¥163.97 and pay additional workload migration costs of ¥6.70 in one day. This section also justifies the cost of reallocating workload flow to tracking DER outputs is cheaper than using the ESS to track DER outputs. If ESS dispatching supplies residual-workload-induced power consumption, only ¥36.50 profit is gained because of limited capacity and lower electricity price. It is much lower than the optimal results by reallocating the workload flow in EDC 15.

E. Case Considering Inaccurate Workload Predictions

As mentioned in the Section I, prediction of workload and

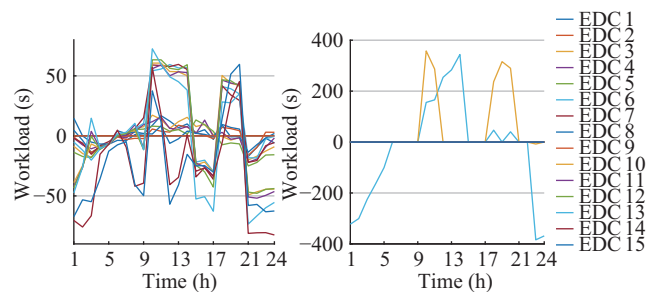


Fig. 9. Workload migration for EDC 9 with $\mu_{BD} = 0\%$ (left) and 5% (right).

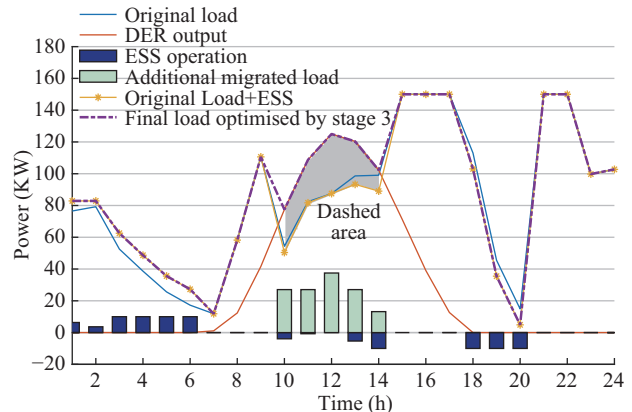


Fig. 10. Original load, DER output, ESS operation and DER tracking results.

DER output could be difficult for EDCs because of their small scale compared with IDCs, thus having the possibility to overload EDCs if unexpected real-time workload increases. The rolling adjustment method in STR, developed in Subsection IV-D, addresses this problem by proportionally sending extra workloads to free servers in nearby EDCs.

As mentioned in Subsection V-A, a number of random computing tasks are added to the EDC cluster as an unexpected workload. Taking the overload condition of EDC 9 at the 10th time slot as an example, overload tasks are required to migrate out from EDC 9 to nearby EDCs, such as EDC 3–7, 10–11 and 13, as shown in Fig. 11. However, at this time EDC 3–5 (connecting by red arrows with EDC 9) are already working at full capacity. Thus, the available migrating target is EDC 6–7, 10–11, and 13, which are connected by green arrows. Nearby EDCs with free servers proportionally share the extra workload in EDC 9 thus all workloads can be successfully processed with a comparatively small delay. This increases the robustness of the STR method working in real-time with further unexpected workload increases.

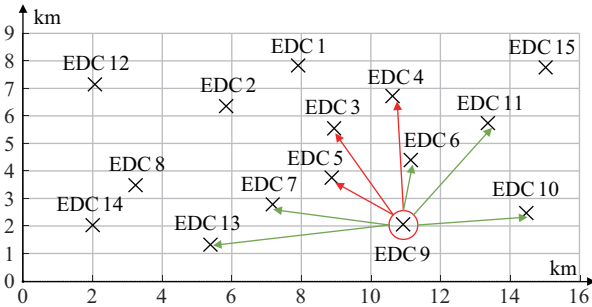


Fig. 11. Geographical workload migration scheme of EDC 9.

Because the rolling adjustment method processes all workload within a safety margin rather than economic operation, efficacy of the STR method to reduce electricity costs is reduced with increasing workload uncertainty. However, even if the uncertainty is increased to 20% of the original workload, the proposed DSCP method can still reduce over 12% electricity costs. Thus, although with a work prediction error of 20%, the proposed method also brings satisfactory benefits to EDC operators.

VI. CONCLUSION

This paper develops a 4-stage STR method to reduce electricity costs in EDC clusters via reallocating workload and ESS capacity between EDCs. The proposed method is demonstrated in an EDC cluster and the results testify to the advantages of the proposed method in reducing electricity costs with strong robustness. Through extensive demonstration, the key observations are:

- Limited literature studied workload migration between EDCs. This work is the first of its kind, it illustrates that, with a rational optimisation method and coordination with ESS, workload migration between EDCs is a practical way to deliver the benefits of energy cost reduction.

- A Bit-Watt transformation, by directly revealing the relationship between power consumption and the amount of computing, reduces decision variables in the workload migration optimization. This could build a mathematical foundation for hybrid modeling of energy systems and communication systems.
- A comprehensive power control method, the STR method, is developed to fully utilize existing resources in EDC clusters to reduce electricity costs. This method consists of 4 stages to provide efficient services. Decoupling of spatial and temporal dimensions in stages 1–3 reduces the dimension of decision variables. The rolling adjustment method in stage 4 enhances robustness of the STR method under high uncertainties in workload forecasting.
- An interesting point found in the simulation is that workload migration cost may have a positive impact on the workload migration operations in EDC clusters. Workload migration cost will bring additional costs to the operators, but it also regularizes and simplifies workload migration schemes in EDC clusters. This can enable EDC operators to obtain simpler and fewer dispatching operations.

REFERENCES

- [1] J. L. Li, C. H. Gu, Y. Xiang, F. R. Li, “Edge-cloud computing systems for smart grid: state-of-the-art, architecture, and applications,” *Journal of Modern Power Systems and Clean Energy*, vol. 10, no. 4, pp. 805–817, Jul. 2022.
- [2] S. C. Li, L. D. Xu, and S. S. Zhao, “5G internet of things: A survey,” *Journal of Industrial Information Integration*, vol. 10, pp. 1–9, Jun. 2018.
- [3] R. Brännvall, M. Siltala, J. Gustafsson, J. Sarkinen, J. Sarkinen, and J. Summers, “EDGE: microgrid data center with mixed energy storage,” in *Proceedings of the Eleventh ACM International Conference on Future Energy Systems*, 2020, pp. 466–473.
- [4] IDCNova. (2020, Nov. 09). Liaocheng, Shandong Province, China launched its first “multi-station integration” edge data center station and put it into operation. [Online]. Available: <http://www.idcnova.com/html/1/59/153/790.html>
- [5] Proximity data centres edge 5 liverpool. [Online]. Available: <https://www.co-lo-x.com/data-centre/proximity-data-centres-edge-5-liverpool/>
- [6] Smart Edge Data Centres Limited. Edge data centres of SmartEdge DC Ltd. [Online]. Available: <https://www.smartedgecd.com/>
- [7] American Tower. Edge data centers. [Online]. Available: <https://www.americantower.com/us/solutions/data-centers/edge/>
- [8] C. Xinhua. The new infrastructure will cause the country’s electricity consumption to soar by nearly 20%, how to deal with it. [Online]. Available: <https://programmersought.com/article/68554776557/>
- [9] Telecommunications Industry Association. (2018). Edge data centers. [Online]. Available: https://www.tiaonline.org/wp-content/uploads/2018/10/TIA_Position_Paper_Edge_Data_Centers-18Oct18.pdf
- [10] L. Rao, X. Liu, M. Ilic, and J. Liu, “MEC-IDC: joint load balancing and power control for distributed internet data centers,” in *Proceedings of the 1st ACM/IEEE International Conference on Cyber-Physical Systems*, 2010, pp. 188–197.
- [11] S. Rahman, A. Gupta, M. Tornatore, and B. Mukherjee, “Dynamic workload migration over backbone network to minimize data center electricity cost,” *IEEE Transactions on Green Communications and Networking*, vol. 2, no. 2, pp. 570–579, Jun. 2018.
- [12] N. H. Tran, D. H. Tran, S. L. Ren, Z. Han, E. N. Huh, and C. S. Hong, “How geo-distributed data centers do demand response: a game-theoretic approach,” *IEEE Transactions on Smart Grid*, vol. 7, no. 2, pp. 937–947, Mar. 2016.
- [13] Y. Y. Shi, B. L. Xu, B. S. Zhang, and D. Wang, “Leveraging energy storage to optimize data center electricity cost in emerging power markets,” in *Proceedings of the Seventh International Conference on Future Energy Systems*, 2016, pp. 18.

- [14] L. Bajracharyay, S. Awasthi, S. Chalise, T. M. Hansen, and R. Tonkoski, "Economic analysis of a data center virtual power plant participating in demand response," in *Proceedings of 2016 IEEE Power and Energy Society General Meeting*, 2016, pp. 1–5.
- [15] J. J. Zhao, Y. C. Hou, L. Liu, F. Xie, X. Mao, P. Luo, J. X. Wang, Z. Q. Zhang, and J. Deng, "The power control method of data center based on cloud-edge collaboration," *Journal of Physics: Conference Series*, vol. 1754, pp. 012094, Feb. 2021.
- [16] L. Chen, W. W. Zhang, and H. M. Ye, "Accurate workload prediction for edge data centers: Savitzky-Golay filter, CNN and BiLSTM with attention mechanism," *Applied Intelligence*, vol. 52, no. 11, pp. 13027–13042, Sep. 2022.
- [17] S. Q. Li, P. F. Zhao, C. H. Gu, J. W. Li, S. Cheng, and M. H. Xu, "Online battery protective energy management for energy-transportation nexus," *IEEE Transactions on Industrial Informatics*, vol. 18, no. 11, pp. 8203–8212, Nov. 2022.
- [18] What and where are edge data centres? [Online]. Available: <https://stipartners.com/edge-computing/%E2%80%8Bwhat-and-where-are-edge-data-centres/>
- [19] M. Al-Fares, A. Loukissas, and A. Vahdat, "A scalable, commodity data center network architecture," *ACM SIGCOMM Computer Communication Review*, vol. 38, no. 4, pp. 63–74, Oct. 2008.
- [20] C. Lim, "Enhancing robustness of per-packet load-balancing for fat-tree," *Applied Sciences*, vol. 11, no. 6, pp. 2664, Mar. 2021.
- [21] F. Ahmad and T. N. Vijaykumar, "Joint optimization of idle and cooling power in data centers while maintaining response time," *ACM Sigplan Notices*, vol. 45, no. 3, pp. 243–256, Mar. 2010.
- [22] Y. W. Zhang, Y. F. Wang, and X. R. Wang, "Electricity bill capping for cloud-scale data centers that impact the power markets," in *Proceedings of the 2012 41st International Conference on Parallel Processing*, 2012, pp. 440–449.
- [23] R. Tripathi, V. Sivaraman, and V. Tamarapalli, "Distributed cost-aware fault-tolerant load balancing in geo-distributed data centers," *IEEE Transactions on Green Communications and Networking*, vol. 6, no. 1, pp. 472–483, Mar. 2022.
- [24] R. L. Deng, R. X. Lu, C. Z. Lai, T. H. Luan, and H. Liang, "Optimal workload allocation in fog-cloud computing toward balanced delay and power consumption," *IEEE Internet of Things Journal*, vol. 3, no. 6, pp. 1171–1181, Dec. 2016.
- [25] NASA-HTTP. HTTP requests to the NASA Kennedy Space Center WWW server in Florida. [Online]. Available: <ftp://ita.ee.lbl.gov/html/contrib/NASA-HTTP.html>



Junlong Li received the B.Eng. degree in the College of Electrical Engineering, Sichuan University, Chengdu, China, in 2019, and the Ph.D. degree from the University of Bath in 2023. He is now working as a researcher with the State Grid Energy Research Institute Co., Ltd., Beijing, China. His main research interests include energy and electricity price, power market, edge-cloud computing in power systems, energy management system, and energy system economics.



Chenghong Gu received a Bachelor's degree from the Shanghai University of Electric Power, Shanghai, China, in 2003, and Master's degree from Shanghai Jiao Tong University, Shanghai, China, in 2007, both in Electrical Engineering. He received a Ph.D. degree from the University of Bath, U.K. He is currently a Reader with the Department of Electronic and Electrical Engineering, University of Bath. His major research interests include multi-vector energy systems, resilience, and power economics.



Lurui Fang joined XJTLU, China, in 2021. He is currently a Lecturer with the E.E. department. His research includes data analytics for power distribution systems and network congestion. He received his B.Eng. degree in Electrical Power Engineering at Chongqing University of Science and Technology, China, in 2013, the MSc degree in Electrical Power Engineering at the University of Southampton, UK, in 2014, and the Ph.D. degree from the University of Bath, UK, in 2021.



Xiangyu Wei received the B.Eng. and B.S. degrees in College of Electrical Engineering from Sichuan University, Chengdu, China, in 2019 and 2023. He is currently pursuing the Ph.D. degree in the Department of Electrical and Computer Engineering, the University of Macau, Macao, China. His research interests include forecasting, dispatching and operation of clean energy.



Yuanbin Zhu received the B.Eng. degree from North China Electricity Power University, China, and the University of Bath, U.K., in 2017, the M.sc. degree from the University of Bath in 2018, and the Ph.D. degree from the University of Bath in 2024. He is now working as a postdoctoral fellow in the China Energy Engineering Group Guangdong Electric Power Design Institute. His research interests include power system analysis and planning, artificial neural network, output forecasting of renewable energy and off-shore wind farm.



Yue Xiang received the B.S. degree in Electrical Engineering and its Automation, and Ph.D. degree in Power System and its Automation from Sichuan University, China, in 2010 and 2016, respectively. Currently, he is a professor at the College of Electrical Engineering, Sichuan University, China. His main research interests are power system planning and optimal operation, low carbon integrated energy systems, electricity market.